REPORT DOCUMENTATION PAGE

Public reporting burden for this collection of information is estimated to average 1 hour per response, including the time for reviewing instructions, searching existing data sources, gathering and maintaining the data needed, and completing and reviewing the collection of information. Send comments regarding this burden estimate or any other aspect of this collection of information, including suggestions for reducing this burden, to Washington Headquarters Services, Directorate for Information Operations and Reports, 1215 Jefferson Davis Highway, Suite 1204, Arlington, VA 22202-4302, and to the Office of Management and Budget, Paperwork Reduction Project (0704-0188), Washington, DC 20503.

1. AGENCY USE ONLY (Leave blank)	2. REPORT DATE	3. REPORT TYPE AND DATES COVERED
	8.Feb.99	THESIS

4. TITLE AND SUBTITLE
VELOCITY FIELD OVER DELTA WINGS AT HIGH ANGLES OF ATTACK

5. FUNDING NUMBERS

6. AUTHOR(S)
2D LT O'DOWD DEVIN O

7. PERFORMING ORGANIZATION NAME(S) AND ADDRESS(ES)
UNIVERSITY OF WASHINGTON

8. PERFORMING ORGANIZATION REPORT NUMBER

9. SPONSORING/MONITORING AGENCY NAME(S) AND ADDRESS(ES)
THE DEPARTMENT OF THE AIR FORCE
AFIT/CIA, BLDG 125
2950 P STREET
WPAFB OH 45433

10. SPONSORING/MONITORING AGENCY REPORT NUMBER
FY99-81

11. SUPPLEMENTARY NOTES

12a. DISTRIBUTION AVAILABILITY STATEMENT
Unlimited distribution
In Accordance With AFI 35-205/AFIT Sup 1

12b. DISTRIBUTION CODE

13. ABSTRACT (Maximum 200 words)

19990219131

14. SUBJECT TERMS			15. NUMBER OF PAGES
			16. PRICE CODE

17. SECURITY CLASSIFICATION OF REPORT	18. SECURITY CLASSIFICATION OF THIS PAGE	19. SECURITY CLASSIFICATION OF ABSTRACT	20. LIMITATION OF ABSTRACT

Velocity Field Over Delta Wings at High Angles of Attack
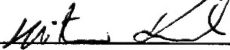
by

Devin O. O'Dowd

A thesis submitted in partial fulfillment
of the requirements for the degree of

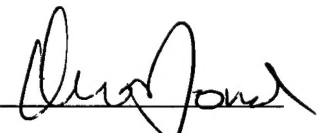Master of Science in Aeronautics and Astronautics

University of Washington

1998

Approved by _____
(Chairman of Supervisory Committee)

Program Authorized
To Offer Degree   Aeronautics and Astronautics

Date _____ August 19, 1998

In presenting this thesis in partial fulfillment of
the requirements for a Master's degree at the
University of Washington, I agree that the Library
shall make its copies freely available for inspection.
I further agree that extensive copying of this thesis
is allowable only for scholarly purposes, consistent
with "fair use" as prescribed in the U.S. Copyright
Law. Any other reproduction for any purposes or by
any means shall not be allowed without my written
permission.

Signature _____

Date __21 aug 98_____

University of Washington

Abstract

Velocity Field Over Delta Wings at High Angles of Attack

By Devin O. O'Dowd

Chairman of Supervisory Committee:
Professor Mitsuru Kurosaka
Department of Aeronautics and Astronautics

Water tunnel experiments were conducted to understand
the nature of vortex breakdown over delta wings at high
angles of attack and at various yaw angles. Two delta
wings with the same sweep angle but different chords and
slightly different thicknesses were placed inside the water
tunnel. Experiments were conducted using two techniques,
Laser Induced Fluorescence (LIF) and Particle Image
Velocimetry (PIV).

Results showed that the core flow experiences an
increase in velocity until breakdown followed by a sharp
decrease in velocity. As the angle of attack increases,
the core flow inside the vortices slows down, in general,
and the strength of the vortices increases. As yaw
increases, the windward side vortex increases in strength
and moves upstream while the leeward side vortex decreases
in strength and moves downstream. At a critical yaw angle,
the leeward side vortex leaves the plate and this vortex
neither leaves the plate, nor experiences an increase in
velocity such as the windward vortex does.

Table of Contents

List of Figures

List of Tables

List of Symbols

c   Chord

u   Stream-wise Velocity

v   Lateral Velocity

V   Velocity

x   Stream-wise Direction

x/c Chord Position in Percentage of Chord

y   Lateral Direction

z   Vertical Direction

α Angle of Attack

β Yaw Angle

ω Vorticity

Subscripts

inf   Upstream Conditions

x   Stream-wise Direction

y   Lateral Direction

z   Vertical Direction

Acknowledgments

Chapter 1: Introduction

The study of vortex breakdown over delta wings at high
angles of attack (AOA) has been an interest to researchers,
mathematicians, and aircraft designers for decades. It is
a very hot topic as it relates to many aircraft being
designed today and because no complete understanding
exists. Most of the understanding that does exist comes in
the form of the problems associated with vortex breakdown.
Many question if it is possible to control the breakdown to
avoid the problems and to aid the aircraft in
maneuverability. The purpose of this study is to lay the
foundation for future research at the University of
Washington, so that the identity to the cause of the vortex
breakdown may be found.

Before discussing the results of the present research,
an awareness of what vortex breakdown is, the problems

associated with it, and how it can be used to improve the aircraft is necessary.

1.1 Definition

At any angle of attack (even near zero AOA), delta winged aircraft experience the formation of a pair of leading edge vortices over the suction side of the wing. These vortices wrap around the apex from the pressure side to the suction side of the wing, while keeping their momentum in the axial direction. This wrapping combined with the axial movement of the fluid creates vortices that resemble a spring.

As the angle of attack increases, the velocity on the suction side of the wing decreases, allowing for these organized and energetic vortices to compress, much like compressing a spring. At high AOA, the compressed spiral shear layer is forced to seek relief by expanding radially. This radial expansion is the breakdown, or bursting. Two types of breakdown are spiral and bubble. Encapsulated within the spiral or bubble is a limited region of flow reversal near the vortex centerline.

1.2 Understanding the Theory

Most engineers claim they understand the theory behind the breakdown, as the majority of the articles published confirm this. Others claim that no understanding exists. One article from 1977 said that "the embarrassing number of different theoretical notions has not, it must be admitted, led to satisfactory understanding of the flows observed" (Faler, 1977). Even a recent article states that "a comprehensive theory of vortex breakdown still does not exist" (Spall, 1996).

Whether the theory is known or not, the problem does exist and must be solved. However, the first step at solving the problem is to understand the nature of the vortices at different situations. An aircraft must be able to maneuver in six degrees of freedom. An understanding of the vortices must be sought at some of these maneuvering conditions. With any success, the engineer will be able to control these vortices so as to avoid the problems associated with vortex breakdown and perhaps even take advantage of the breakdown. The engineer will also be able to achieve controllable maneuver at high AOA for both steady and unsteady situations.

Many claims have been made as to the physics of the
flow field over the surface of the wing. Several
instabilities have been identified as relating to the
leading-edge vortex flow field. Gadel-Hak and Blackwelder
(1985) identified discrete vortices from the leading edge
of the delta wing that convect around the primary vortex
after they emanate from the leading edge of the wing.
Payne (1988) and Shi (1987) have also observed this
instability. These researchers attributed the emergence of
these small-scale vortices to the Kelvin-Helmholtz type
instability.

Another observation was the appearance of a stationary
longitudinal instability which they associated to the
curvature of the separated shear layer (Lowson, 1995).
Visbal and Gordnier confirmed this observation in their
Navier-Stokes computational study and claimed that this
unsteady vortex shedding is triggered by the interaction
between the primary vortex and the surface of the wing.

Though many observations and claims have been made,
the true identity to the cause of the vortex breakdown is
not fully known.

1.3 Problems with Breakdown

At high AOA, these organized and energetic vortices breakdown (burst), causing many problems. One problem is the vortices lose their effectiveness to generate high normal forces after developing the large-scale instabilities. This is not a suitable condition for an aircraft that requires these forces to fly.

Another problem is that the burst vortices generate large buffeting problems on the wing. This is probably one of the most infamous problems. These problems have become evident on such delta-winged aircraft as the F-22 and Joint Strike Fighter (JSF).

Other problems that engineers have noticed is that the breakdown leads to aircraft motion instabilities, the hysteresis phenomena, and cross coupling between various degrees of freedom of the motion of the aircraft (Shih 1996).

Solving the problem means the minimizing of the damage placed on the aircraft due to breakdown and the better operation of the aircraft.

1.4 Present Study

The present study will look at the location of the breakdown and the velocity and vorticity patterns of a delta wing at various angles of attack (AOA). Much research has been done in the area of vortex breakdown at various AOA. However, fewer studies have used the Particle Image Velocimetry (PIV) technique, and fewer still have introduced yaw into the research. This study will use the PIV technique and a flow visualization technique to analyze the velocity and vorticity of a delta wing at various AOA and various yaw angles.

Chapter 2: Experimental Facility and Techniques

The study of the velocity field and vorticity pattern was performed using two methods. Laser Induced Fluorescence (LIF) was used to provide flow visualization. Particle Image Velocimetry (PIV) provided a two-dimensional velocity field and the corresponding vorticity perpendicular to the two-dimensional plane. This chapter describes the water tunnel facility and the set-up for both the LIF and PIV techniques.

2.1 Water Tunnel and Jet Supply System

The University of Washington Water Tunnel Facility is a recirculating tunnel with a 3.0m x 0.7m x 0.7m glass test section. It has a maximum flow speed of 70 cm/s. A sketch of the water tunnel is shown in figure 2-1. The paper by Eroglu (1991) contains a complete description of the water tunnel. A free stream turbulence level of approximately

0.3% of the mean flow existed for all tunnel speeds.

Except for the water tunnel velocity calibration, all

experiments were conducted at 3.83 cm/s.

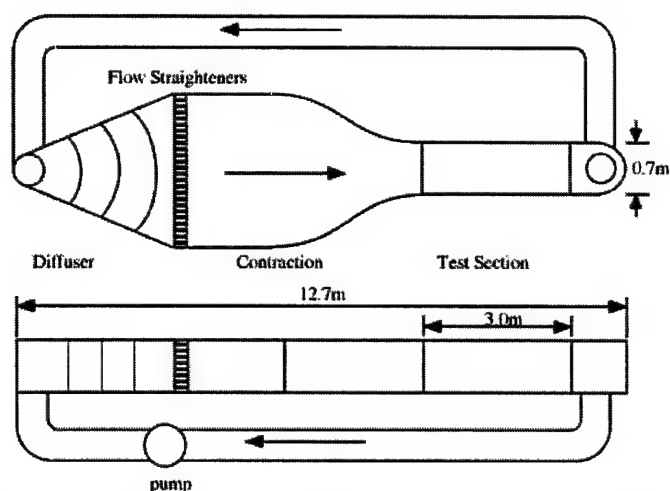**Figure 2-1**: University of Washington Water Tunnel Facility

Two acrylic flat plated delta wings of different sizes
were suspended in the test section midway between the
surface of the water and the bottom of the tunnel. The
subsequent chapter gives a more detailed description of the
two wings. The wings were supported by a 0.63cm x 4cm
piece of aluminum 6 cm aft of the wing, as seen in the
following figure.
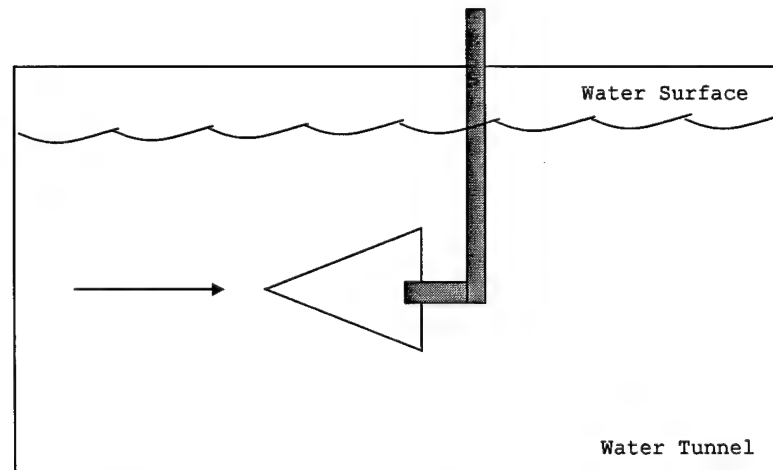
Figure 2-2: Support of Delta Wings

The jet fluid for the LIF experiments consisted of 2×10^{-4} grams of Disodium Fluorescein per liter of water. The jet fluid for the PIV experiments consisted of 3 Tbsp. 1 μm diameter nylon particles with specific gravity 1.02.

A control pump was used to control the pressure at which the jet flow was emitted. An injector was placed at various places in the flow, from 20 cm upstream to the apex. A discussion on the impact of the injector placement is discussed in the subsequent chapter. The injector used had a 1 mm diameter hole.

2.2 Laser Induced Fluorescence Technique

The laser induced fluorescence technique uses a laser sheet generated by an 8 watt argon-ion laser (Spectra Physics

Model 2020-5) and a light sheet probe (TSI Model 9855-32)
to illuminate the jet fluid. With no lights, the
fluorescence is invisible to the naked eye; with the laser
sheet, the fluorescence is excited to illumination. A
digital video camera recorded the flow and Adobe Premiere™
was used to store the images on the computer as individual
pictures. Adobe Photoshop™ was then used to crop the
pictures and to invert them. The pictures are black with
neon-green colored fluorescence revealing the streamlines.
In the ensuing chapter, the images were inverted so that
the colors were not as dark.

The laser sheet was oriented along two different
planes. It was aligned both parallel and perpendicular to
the plate. The parallel view captured the core flow from
the apex to the end of the plate. The perpendicular view,
or transverse view, captured the vortex core plane, or
cross-section of the vortex, at a given chord-wise
position.

By shining the laser parallel to the suction side of
the wing, and giving the camera a direct line of sight, the
core flow was captured. The vortex core plane was much
more difficult to capture, as a mirror had to be used to
capture the images. Though there was no other solution,

the mirror diminished the accuracy of the results.

Figures 2-3 and 2-4 show the laser sheet orientations for

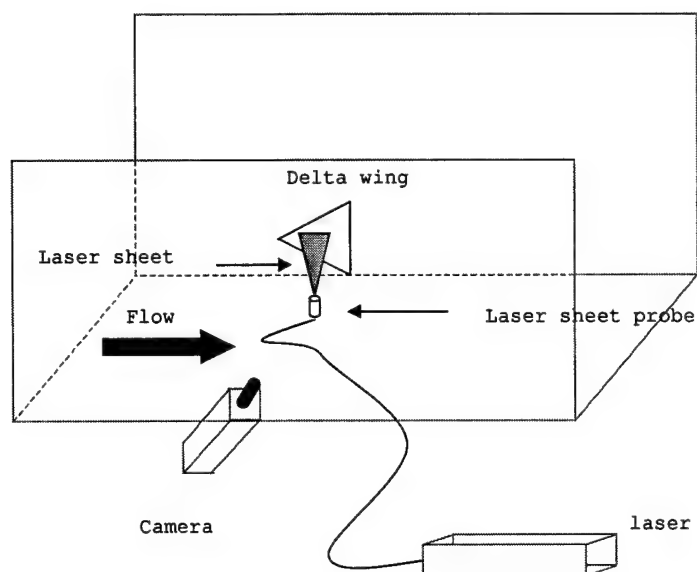the core flow and vortex core plane, respectively.
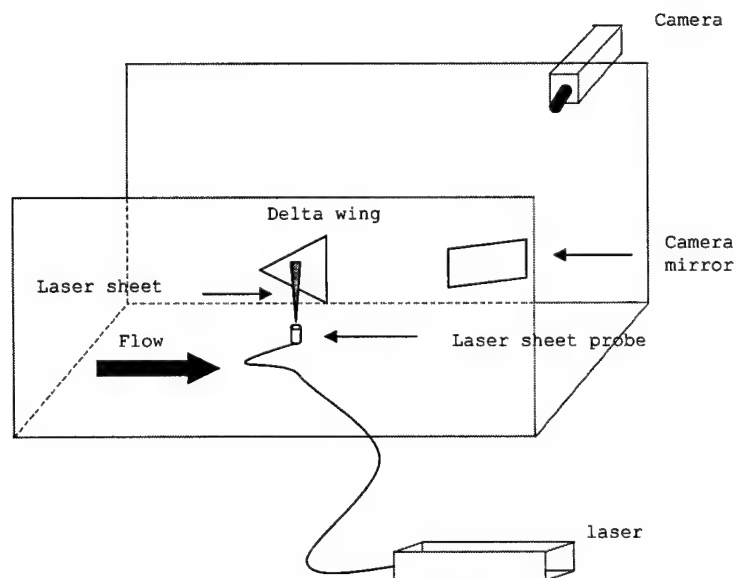

Figure 2-3: LIF Set-up, Core Flow

Figure 2-4: LIF Set-up, Vortex Core Plane

2.3 Particle Image Velocimetry Technique

Quantitative flow field measurements were acquired using a TSI Incorporated Particle Image Velocimetry (PIV) system. Advantages to PIV are that it does not obstruct the flow and it gives a two-dimensional result. This technique allows for the simultaneous acquisition of hundreds of velocity vectors. The laser sheet is used to illuminate nylon particles and the particle images are recorded using a CCD camera and saved on a computer. The CCD camera records each laser pulse on separate video frames and a cross-correlation algorithm can then be run on each pair of images to determine the particle displacement. The laser sheet orientations used are identical to those used during LIF.

The PIV system consists of a laser, beam modulator, synchronizer, laser sheet probe, camera, and computer as shown in figure 2-5. The laser beam passes through a collimating lens into the beam modulator (TSI Model 620010), which uses the first order beam to turn the laser on and off. The TSI Instruction Manual is much more specific in the set-up of the modulator. A 40 MHz signal from the synchronizer (TSI Model 610030) controls the beam modulator. The synchronizer provides the signal control

for both the camera and beam modulator. Table 2-1 lists

the synchronizer settings used for the cross-correlation of

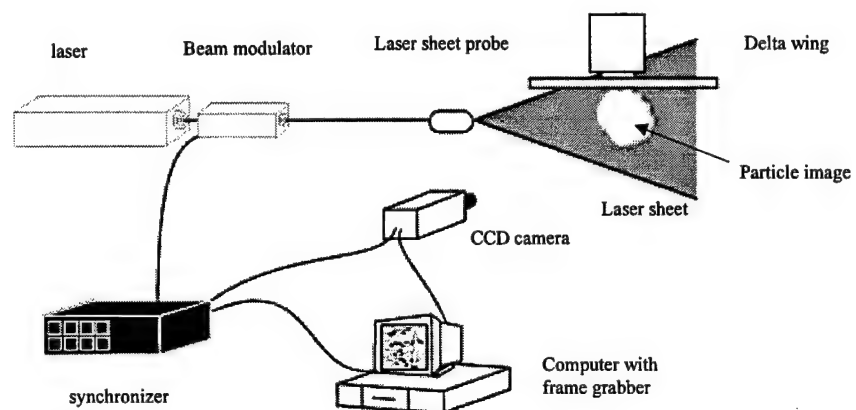two video frames (modified from TSI PIV Instruction Manual,

1995).

Figure 2-5: Particle Image Velocimetry Set-up

Table 2-1: Synchronizer Set-up

Synchronizer Button	Parameter Settings	Description of Parameter
Pulse		
Mode	Pulse Mode Double Pulse	Generates two pulses at the programmed separation time
Laser Type (2nd Function)	Argon	Type of laser used
Duration	Pulse Duration 50% Duty Cycle	Time the laser is on during a pulse (percentage of the pulse separation time – 50% maximum)
Separation	Pulse Separation 0.01 sec 0.02 sec	Separation between two consecutive pulses (10 ms for core flow, 20 ms for vortex core plane)
Camera		
Mode	Video Camera Triggered	Allows the camera to be the time master
# of Frames	00 Frames	Camera is fired continuously until RUN/STOP button is pressed
Frame Rate	N/A	Does not apply to video triggered mode
Pulse Delay (2nd Function)	Pulse Delay Time 42.5 ms 35.0 ms	Used with Pulse Separation (10 ms, 20 ms respectively). See Instruction Manual, pg. 4-4, for approximate pulse delays for other pulse separations
External		
Start	00 Seconds	
Stop	00 Seconds	
Trigger		
Run/Stop		Activates laser pulsing
Int/Ext	Trigger Source Internal	Set to internal when no image shifting is being used

The CCD camera (TSI Model 630044) has a frame rate of 30 frames per second and a resolution of 640 pixels x 480 pixels. The camera has a Nikon Macro lens (AF Micro Nikkor, 105 mm, f/2.8D) with maximum magnification of 10:1.

Two different images can be recorded on the order of 0.02 ms apart and a total of 13 consecutive images can be stored in the frame grabber memory.

The computer is a 90 MHz Pentium equipped with two TSI software packages: Insight™ and Datashow™. Insight™ is responsible for the acquisition and processing of the particle displacements from the raw image data while Datashow™ is used for the post-processing of the pixel displacement fields (in order to remove the obviously bad vectors and to average with other image pairs to remove noise). Details on the use and set-up of Insight™ and Datashow™ can be found in Haven (1996). The velocities and vortices associated with the displacement fields were processed by the software package Spyglass Transform™. This program converted the data into velocities and vortices using finite differencing to approximate $\frac{\partial v}{\partial x} - \frac{\partial u}{\partial y}$.

Before using the Insight™ and Spyglass Transform™, the interrogation grid size had to be determined, which is dependant on the particle displacement, velocity, pulse separation time, and pulse delay time. For the core flow, the picture was divided up into a 30x30 grid. For the

vortex core plane, the picture was divided up into a 40x40 grid. This information was used when processing the data in Insight™.

The dimensions of the picture viewed by the camera also had to be determined. These dimensions were entered into a Spyglass Transform™ macro that converts the velocity from pixels per second to centimeters per second.

Chapter 3: Experimental Results

A combination of Laser Induced Fluorescence (LIF) and
Particle Image Velocimetry (PIV) was used to investigate
the behavior of the leading edge vortices, also known as
apex vortices. These vortices were observed both looking
down onto the top of the wing (which shows the vortex
lines), which is labeled parallel plane; and from the rear
of the wing (which shows the cross view), which is labeled
transverse plane.

For the majority of experiments, the water tunnel was
run at 3.8 cm/s. Faster and slower velocities were
desired, but caused problems. If the tunnel is any slower,
the bearings in the motor begin to vibrate and the flow
becomes less steady and increases the amount of
fluctuations in the velocity.

If the tunnel is any faster, the camera will not be
able to see the particles as they are moving to fast to

accurately measure their displacement. To observe faster particles (especially in the transverse plane), the separation time and pulse delay times must be short. However, the shorter the time, the less power the laser produces and consequently, the laser is not bright enough for the particles to be reflected. Thus, one conservative value for the velocity was chosen.

The research involved finding the flow field over the delta wing. This includes velocity. The program Spyglass Transform™ was used to calculate the velocities of the flow based on particle displacement in centimeters. A calibration of the system with Spyglass Transform™ was first performed to relate the velocity that Spyglass Transform™ gives to the free stream flow.

3.1 Velocity Calibration

Before placing any obstruction into the flow (e.g. delta wing), PIV measurements of the free stream flow were taken. For steady, one-dimensional flow, water tunnel velocities tested were between about 2.5 cm/s and about 15 cm/s. The camera did not have any problems in viewing the particles.

With variable water tunnel velocities, PIV measurements were taken and were processed through Spyglass

Transform™ to obtain their velocity. The flow proved to be very uniform and one-dimensional and the velocities from Spyglass Transform™ were very close to constant. Comparing these given values for velocities with the water tunnel speed (which was provided with the tunnel and verified by Maj. Brenda Haven using PIV), a linear relationship was observed. Using Microsoft Excel, which uses a least squares fit to form trendlines, the equation of the line was calculated. The results were again verified by running the same experiments with a different size flow field. Initially, the flow field viewed by the camera was 4 cm by 3 cm. The flow field viewed was changed and the equation proved to be quite good. Figure 3-1 shows the two different setups, corresponding to the initial and subsequent flow field views, and the compared relationship between the water tunnel velocity and the velocity measured by Spyglass Transform™.
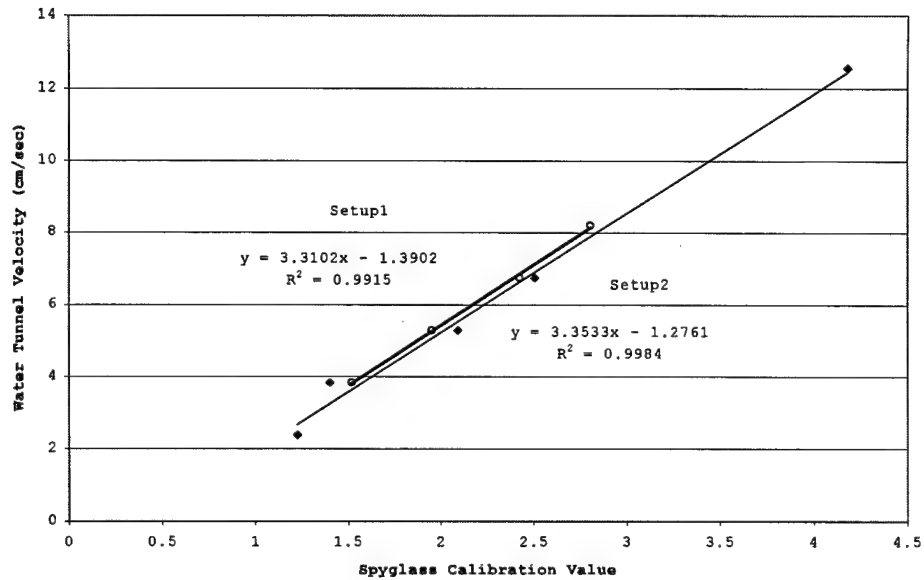
Figure 3-1: PIV Calibration Conversion

During later experiments, the non-dimensional velocities from Spyglass Transform™ would be converted into cm/s.

After processing data, negative velocities were found. This would be acceptable within the region of breakdown. However, at the apex where the flow is traveling downstream, negative velocities (which indicates flow traveling upstream) appeared. The conclusion made was that the equation of the trendlines is true only for steady, uniform, one-dimensional flow. With a wing at some angle of attack, the flow will have non-uniformities and the calibration equation will not give accurate results. Also, the two-dimensional laser sheet cannot provide accurate results for three-dimensional flow. Another problem is

that Spyglass Transform™ uses a Macro that can give
inaccuracies when converting from pixels per second to
centimeters per second, especially when the camera is moved
and the picture viewed by the camera has changed. All of
these factors contribute to the inaccurate results. For
this reason, the calibration factor will not be applied in
this research.

Care must be taken in future research to find an
accurate relationship between the velocity provided by
Spyglass Transform™ and the actual velocity. For this
study, the upstream velocity, V_{inf}, that is provided by
Spyglass Transform™ normalized the velocities in the vortex
core.

3.2 Parallel Plane Flow

After having obtained the equation to convert the velocity
given in Spyglass Tranform™ to cm/s (though this equation
is not be used in this study because of the inaccuracy),
observations on the core flow were made. As it has been
stated previously, few studies of vortex breakdown have
been analyzed using PIV. It is also true that few studies
have looked at the change of yaw on the wing.

Two delta-wings, sketched below, which are similar in shape but different in sizes, are used.
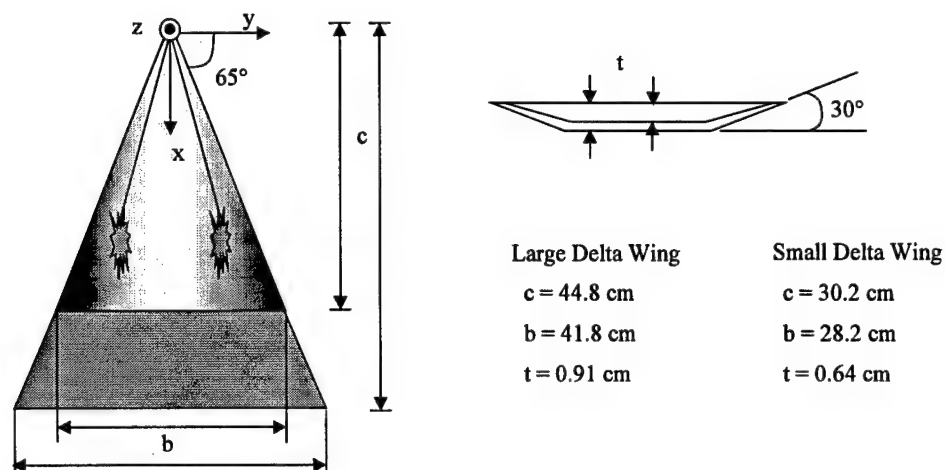

Large Delta Wing
c = 44.8 cm
b = 41.8 cm
t = 0.91 cm

Small Delta Wing
c = 30.2 cm
b = 28.2 cm
t = 0.64 cm

Figure 3-2: Delta Wings Used

These delta wings were placed at different angles of attack, α, and different yaw angles, β, which are shown in the following figure.
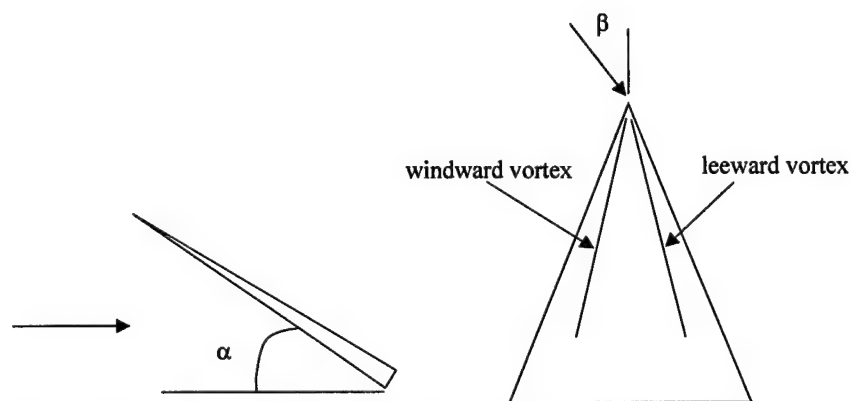

Figure 3-3: Definition of Angles and Vortices

As figure 3-2 illustrates, these two wings are only
different in the root chord and the thickness of the plate.
The small wing has thickness 0.25 in. (0.64 cm, 2.1% chord)
while the large has thickness 0.36 in. (0.91 cm, 2.0%
chord). The sweep angle of 65° is the same for both wings.
A visual test was performed to determine how much of a
difference there was between the large and small wings,
especially with regard to location of the breakdown. It
must first be noted that instabilities in the flow cause
the position of vortex breakdown to scatter within a range
of about 5 cm. The visual test confirmed that for the
large and small delta wings at the same AOA, the vortices
breakdown at almost the same x-position, equidistant from
the apex. Thus, expressed in terms of x/c, the vortex
breakdown positions are different: table 3-1 lists the
location in percentage of chord for each wing at three
different AOA.

Table 3-1: Location of Breakdown

Angle of Attack → Wing ↓	20°	30°	40°
x/c for Small (chord = 30.2 cm)	>80%	40 – 50%	15 – 25%
x/c for Large (chord = 44.8 cm)	>60%	30 – 40%	20 – 30%

Though breakdown does not occur at the exact same distance
from the apex, perhaps due to the difference in thickness

or the exact placement of the injector (where particles or fluorescence is emitted), the two plates show so much similarity that interchanging the plates during the research would not affect results.

In the initial investigation, the large delta wing analyzed. At very low angles of attack, leading edge vortices appear, but generally do not breakdown. The reason for this is because the root chord is not big enough for a breakdown to appear; that after the vortex leaves the trailing edge, it typically diffuses. A large delta wing is beneficial because it allows for the observation of the breakdown at lesser angles of attack (AOA), as compared to a smaller delta wing. However, due to the size of the water tunnel, the wing could not yaw without its apex emerging from the water. For this reason, the smaller wing was used.

Attempts were made to determine the importance of the placement of the injector. The injector was placed upstream in various locations and at the apex on the pressure side of the wing. It was determined that the placement did not affect results significantly. Many requirements for where the injector is placed and how it is used must be considered. First, the pressure at which the

particles or fluorescence is emitted must be low so as
not to induce too much jet flow. Second, the obstruction
of the injector in the flow does cause minor disturbances,
which are difficult to avoid. Third, the placement of the
injector can move the location of the breakdown up to about
five per cent of the chord. With this in mind, it was
concluded that although our results are not perfect, they
do provide powerful insight into the nature of the vortices
and the breakdown. Therefore, for the purposes of this
study, it did not make a difference whether the large wing
or small wing was used.

Baseline conditions were first observed to see how the
vortex acts at various angles of attacks. As the angle of
attack increases, the location of breakdown moves upstream
(as indicated in table 3-1). Also, as the angle of attack
increases, the strength of the vortex increases. Figures
3-4 and 3-5 show the component of vorticity normal to the
x-y plane (ω_z) for an AOA of 20° and 30°, respectively.
What is seen is the two-dimensional look at the flow. The
top regions show negative vorticity (clockwise) and the
bottom regions show positive vorticity (counterclockwise).
The key under each plot shows that a greater angle of
attack has a stronger vortex structure (represented by

magnitude sec^{-1}). The different signs of voriticity indicate a spiral pattern. A sign switch of vorticity, shown in figure 3-6, has been observed by Shih and Ding (1996), but could not be observed in this present study. Presumably, this is due to the limited number of test points (four image pairs) used in making the time-averaged plots.
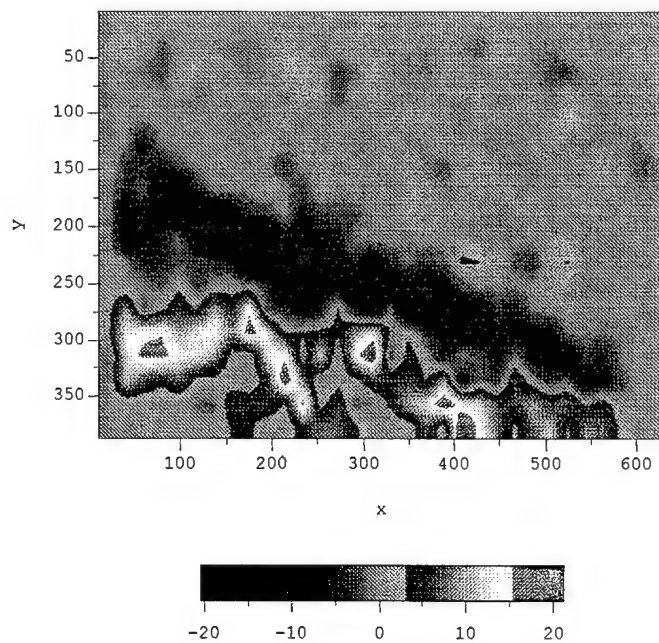

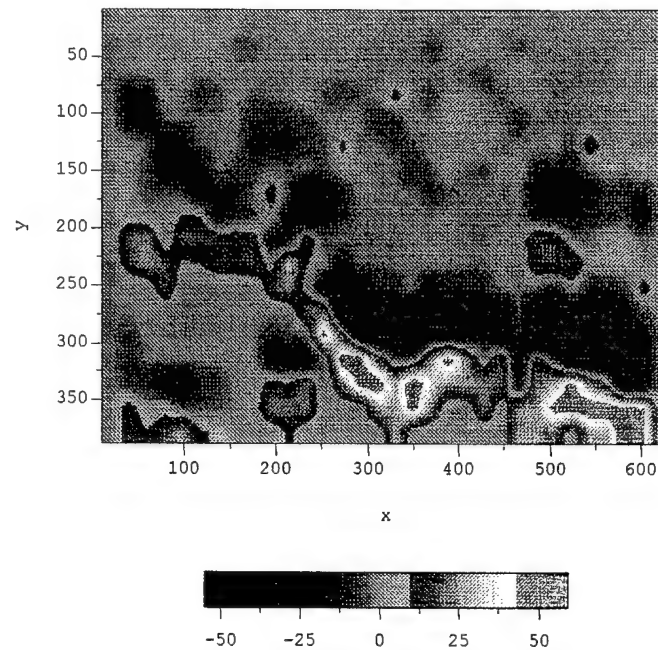**Figure 3-4**: Vortex Strength (ω_z), Core-wise View, $\alpha = 20°$

Figure 3-5: Vortex Strength (ω_z), Core-wise View, $\alpha = 30°$
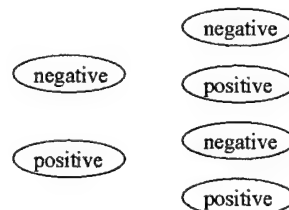

Figure 3-6: Sign Switch of Vorticity

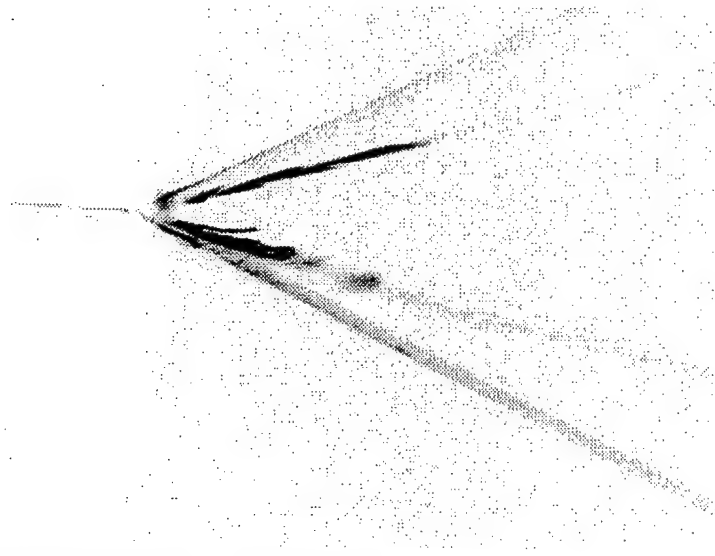LIF pictures that correspond with the figures 3-4 and 3-5 are shown in figures 3-7 and 3-8.

Figure 3-7: LIF Picture, $\alpha = 20°$

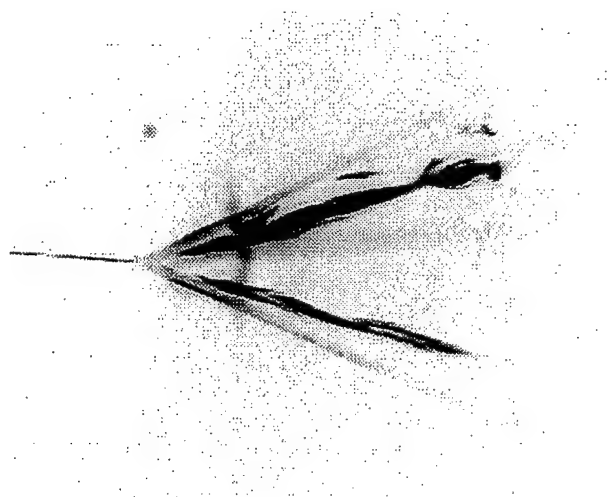**Figure 3-8:** LIF Picture, $\alpha = 30°$

Previous research has shown that the velocity in the vortex core increases to the point at which it breaks down and then a decrease in velocity occurs. The flow can be described as jet flow until breakdown, followed by wake

flow. A study was performed at an AOA of 30° with no

yaw. The large wing was used and the observations were

made on the lower vortex. The LIF picture that corresponds

to this study is found in figure 3-8. A qualitative view

of the vector plot is demonstrated in figures 3-9 and 3-10.

Figure 3-9 is the velocity field from the apex to 25% of

the root chord (0.25c). Figure 3-10 is the velocity field

from the 0.25c to 0.5c. Figure 3-11 is a quantitative look

at the velocity field. Notice that the velocity increases

up to 3 times the upstream velocity, V_{inf}, on the "y-axis"

of figure 3-11. Though the velocities do not correspond

accurately to the velocity given in cm/s, the results show

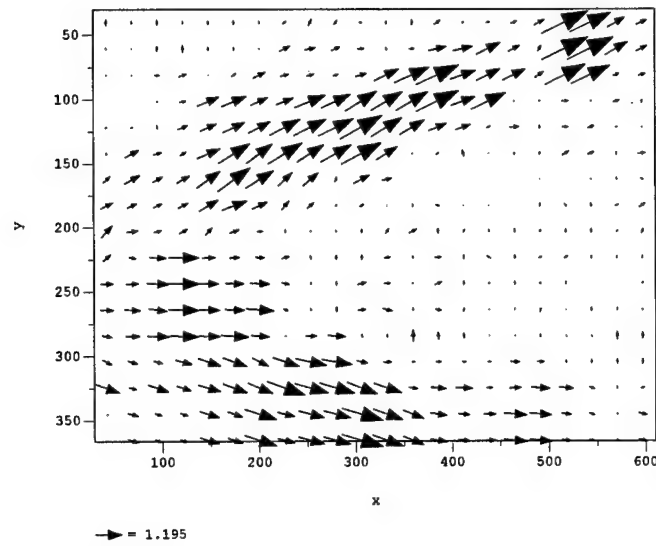both quantitatively and qualitatively how the velocity

behaves over the wing.

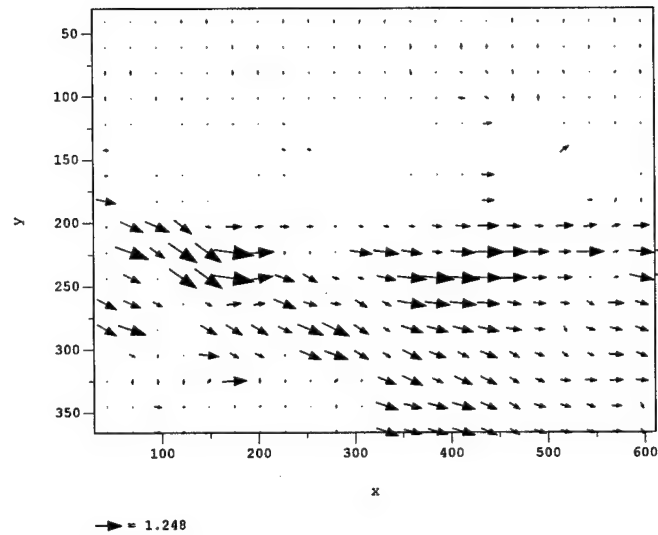**Figure 3-9**: Velocity Field, α = 30°, β = 0°, Apex to 0.25c

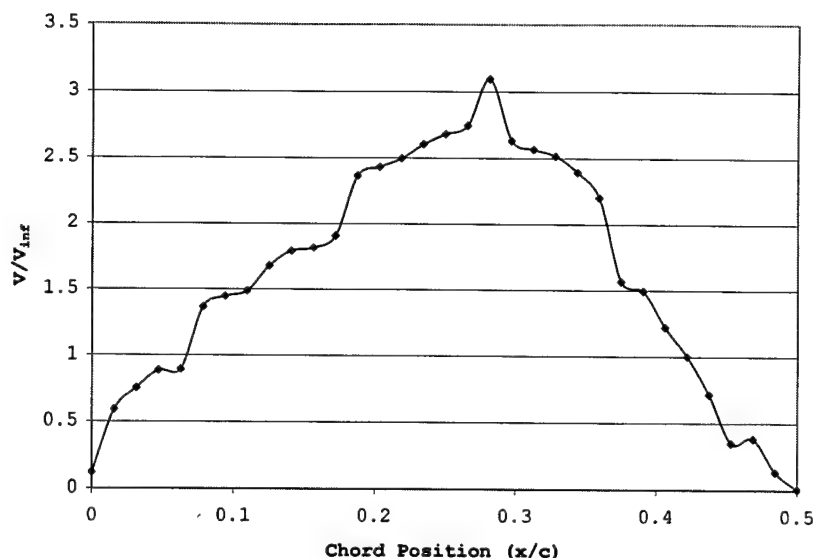**Figure 3-10**: Velocity Field, α = 30°, β = 0°, 0.25c to 0.5c

Figure 3-11: Velocity Field, $\alpha = 30°$, $\beta = 0°$

The results confirmed previous studies (Erickson, 1980 and Shih, 1996). Notice that in figure 3-11, the velocity has a gradual increase in velocity, up to three times the upstream velocity, and at the point of breakdown (about 0.3c), there is a rather sharp decrease in velocity.

The effects due to yaw were then considered. The study attempted to determine whether or not the velocity field looked as it did at zero yaw. It also tried to analyze the point at which the leeward side vortex left the plate and its corresponding velocity field.

Initial observations showed that as yaw increases, the windward vortex breakdown moves upstream while the leeward vortex breakdown moves downstream. Figure 3-12 shows the

LIF picture for 30° AOA and 30° yaw. The top vortex

(leeward side) shows no breakdown while the bottom vortex

(windward side) shows that the breakdown (spiral type) has
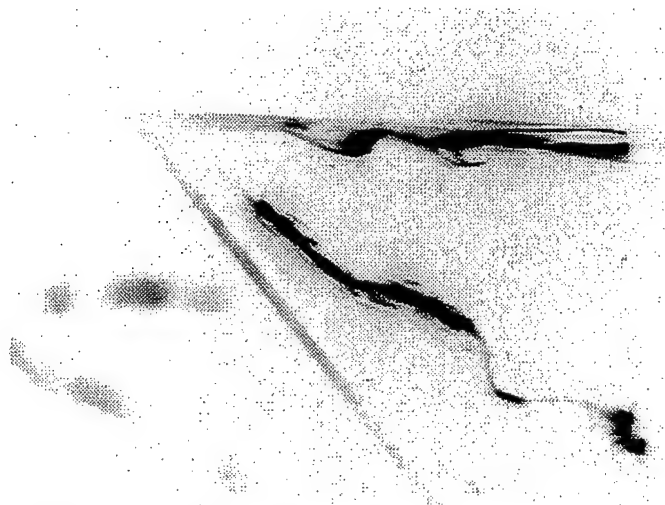
moved upstream.

Figure 3-12: LIF, $\alpha = 30°$, $\beta = 30°$

The next observation made was the point at which the

leeward side vortex moves off the plate. This is seen in

figure 3-13.

Figure 3-13: LIF, $\alpha = 40°$ $\beta = 45°$

Though the plate is hard to see, it is observed that the
leeward side vortex has left the plate. The next study
considered was what the velocity fields look like at the
condition of 30° AOA and 45° yaw. Figures 3-14 and 3-15
show the vector plots for the velocity field of the
windward side vortex. Figure 3-14 corresponds to the apex
to 0.15c and figure 3-15 corresponds to 0.15c to 0.25c
(following the breakdown). Figure 3-16 shows the
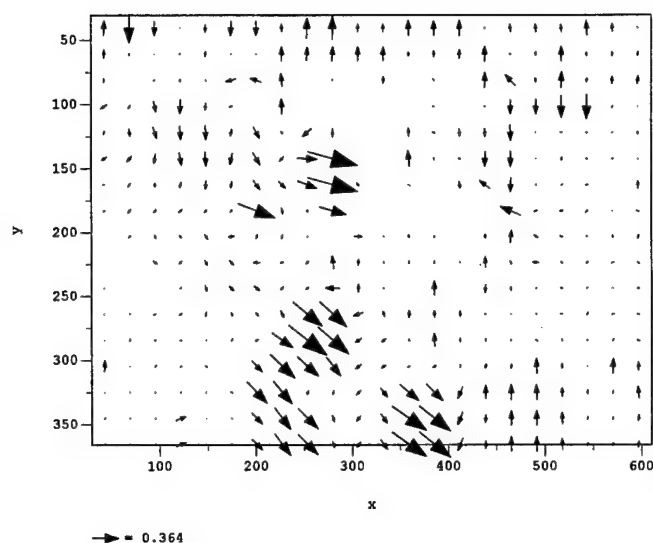quantitative look at the velocity field.

Figure 3-14: Windward Side Velocity Field, α = 30°, β = 45°, Apex to 0.15c

Figure 3-15: Windward Side Velocity Field, α = 30°, β = 45°, 0.15c to 0.25c (Including Breakdown)

Figure 3-16: Windward Side Velocity Field, $\alpha = 30°$, $\beta = 45°$

Notice the similarity to the velocity field with zero yaw as shown in figure 3-11. Also, the maximum V/V_{inf} at a higher yaw angle (approximately 1.9) is less than the maximum V/V_{inf} at zero yaw (approximately 3.1).

When looking at the leeward side vortex, results are much different. Initially, just after the apex, the velocity increases sharply, but steadies out to a very gradual increase. Figures 3-17 through 3-20 are the vector plots for the apex to 0.2c, 0.2c to 0.4c, 0.4c to 0.6c, and 0.6c to 0.8c, respectively. Figure 3-21 shows the quantitative look at the velocity field.

Figure 3-17: Leeward Side Velocity Field, $\alpha = 30°$, $\beta = 45°$, Apex to 0.2c

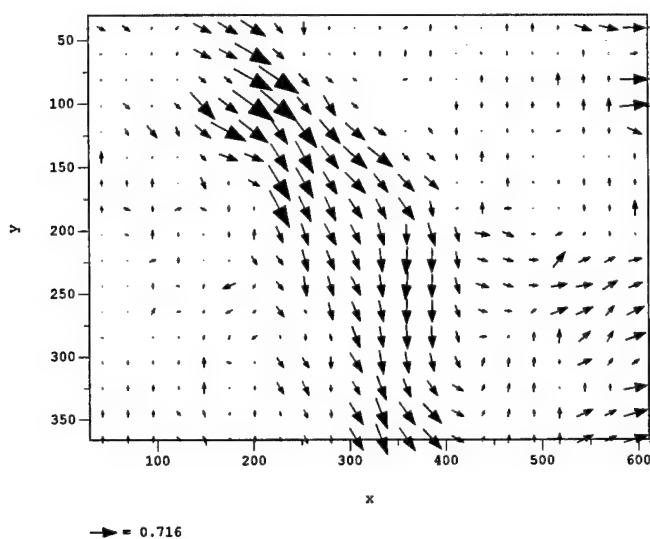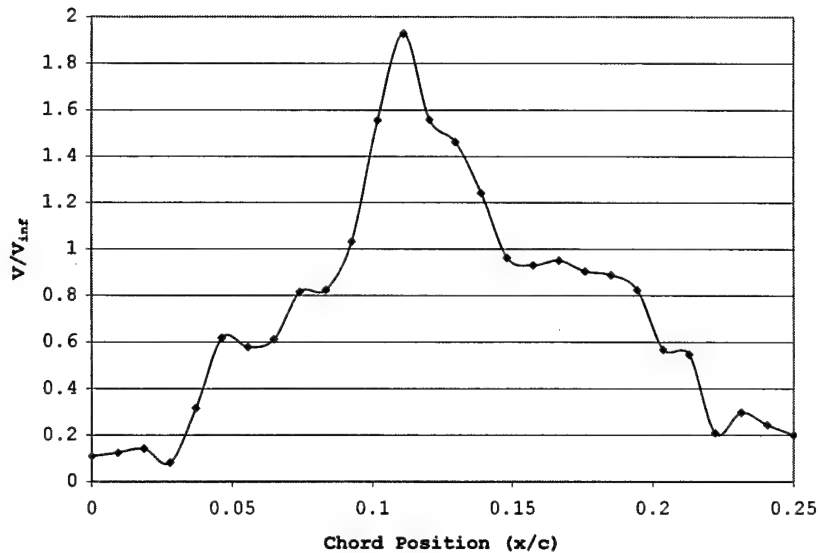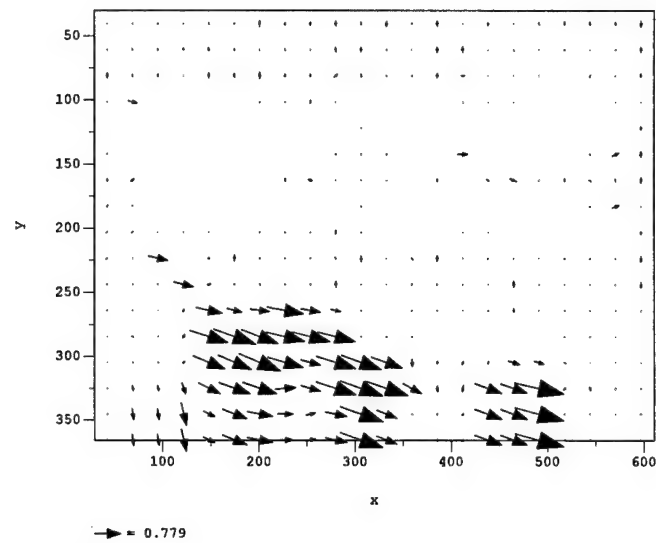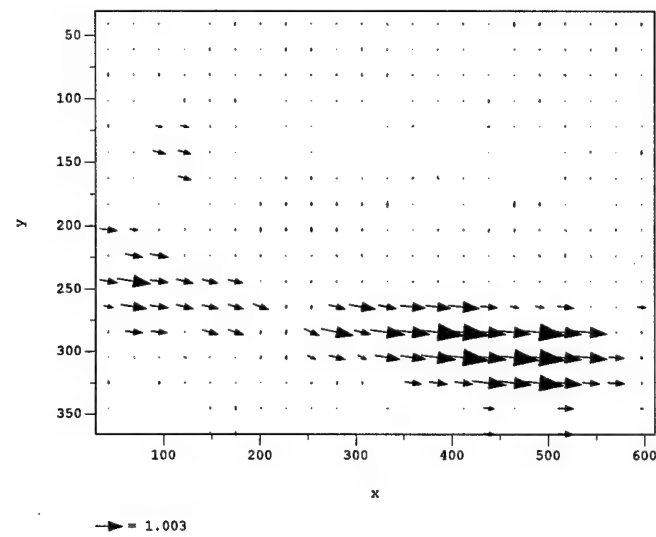**Figure 3-18:** Leeward Side Velocity Field, $\alpha = 30°$, $\beta = 45°$, 0.2c to 0.4c
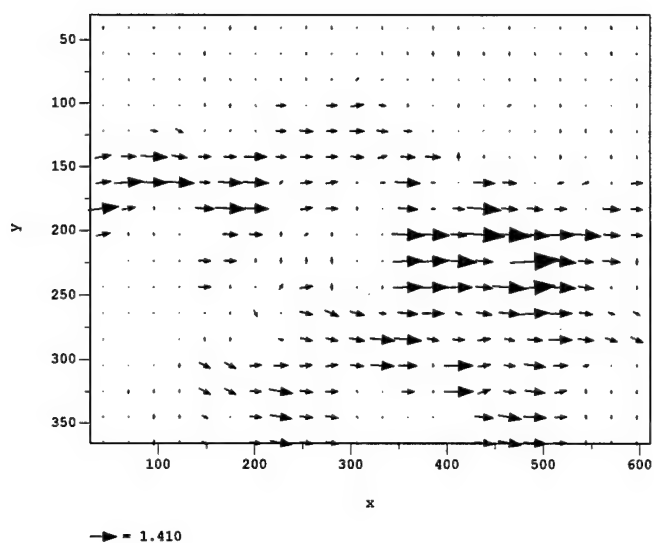
Figure 3-19: Leeward Side Velocity Field, α = 30°, β = 45°, 0.4c to 0.6c
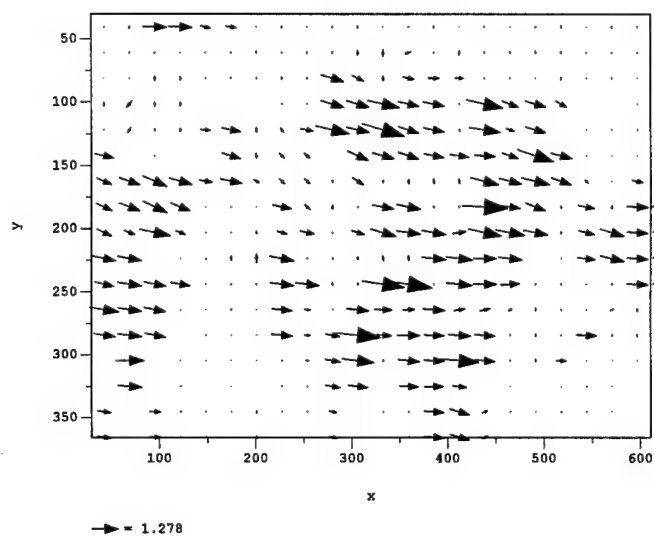
Figure 3-20: Leeward Side Velocity Field, α = 30°, β = 45°, 0.6c to 0.8c
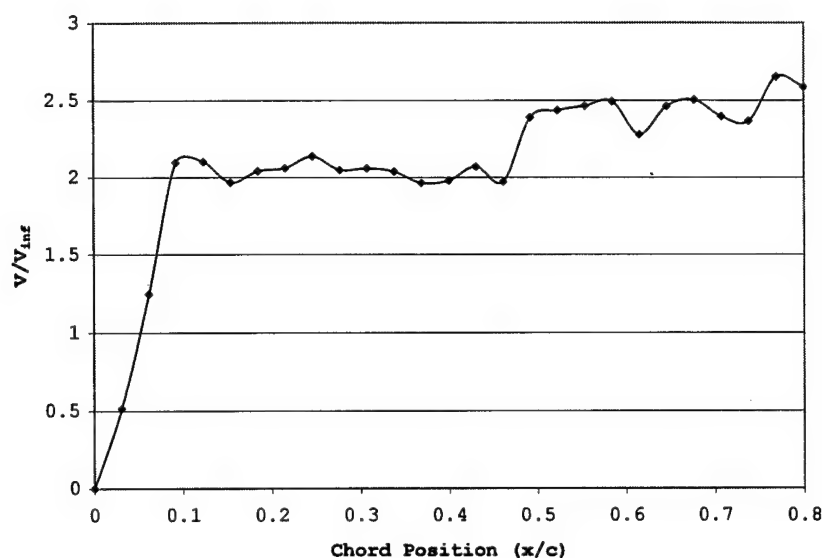
Figure 3-21: Leeward Side Velocity Field for α = 30°, β = 45°

Results show that while the wing is at a high angle of attack and at a high yaw, the leeward vortex core neither speeds up much nor breaks down. The critical yaw angle for the 65° swept wing is between 40° and 45°. At 25° yaw, the leeward side leading edge is parallel to the upstream flow. As yaw increases above 25°, the leeward vortex core moves closer to the leading edge. It is not until the yaw is between 40° and 45° that the leeward side vortex leaves the plate.

β = 25°   β = 40°-45°

Vortex has
left the plate
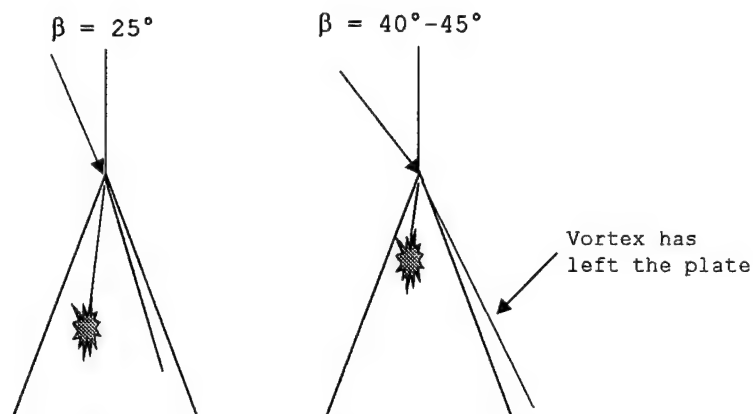
Figure 3-22: Effect of Yaw Angle on Leeward Vortex Core

Other observations from this study noted is the asymmetry that occurs over the plate, even at zero yaw. It is evident from the following figure that even though the experiment should involve no asymmetric results, they appear nevertheless.
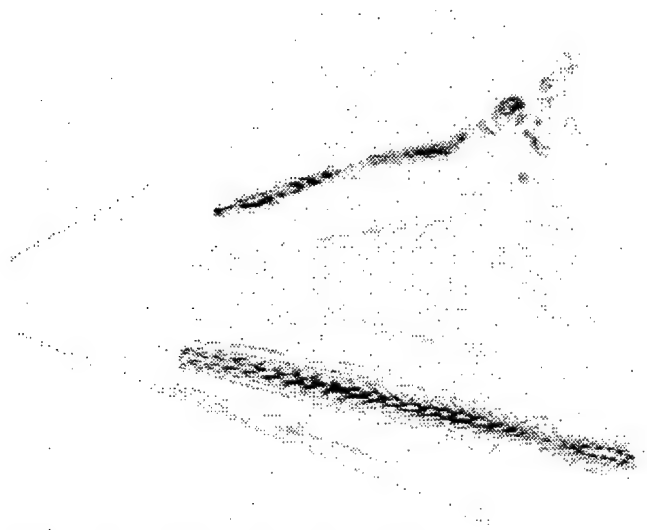
Figure 3-23: Asymmetry in the Flow

Reasons for asymmetry can include the placement of the injector, vortices that develop in the jet supply system, obstructions in the flow, and the presence or absence of a free surface. Obstructions include the support for the wing, even though it is located downstream of the wing.

For future research in studying the core flow, the velocities given by Spyglass Transform™ must be recalibrated to account for non-uniform flow as best as possible. To be more accurate, future studies must make sure the camera is focused in on smaller regions with many particles and a bright laser to reflect the particles. For this baseline study, though not as accurate in magnitudes, results in the form of trends were very helpful.

3.3 Transverse Plane

When considering the core-wise flow in the previous section, observations were made on the vorticity (see figures 3-4 and 3-5. In later studies, observations were made of the vorticity on the cross section of the vortex core. That is, the camera was pointed from downstream to upstream, with line of sight parallel to the vortex, using a mirror. The view that the camera sees is sketched below.
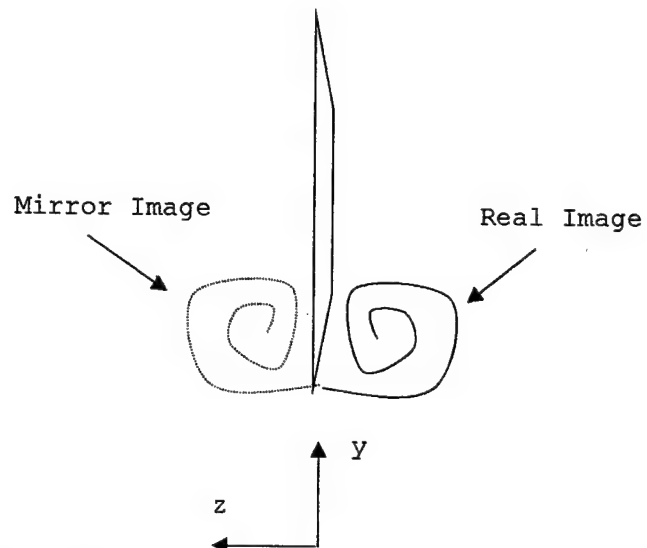
Figure 3-24: Sketch of Transverse Plane View

A sample image is shown below.
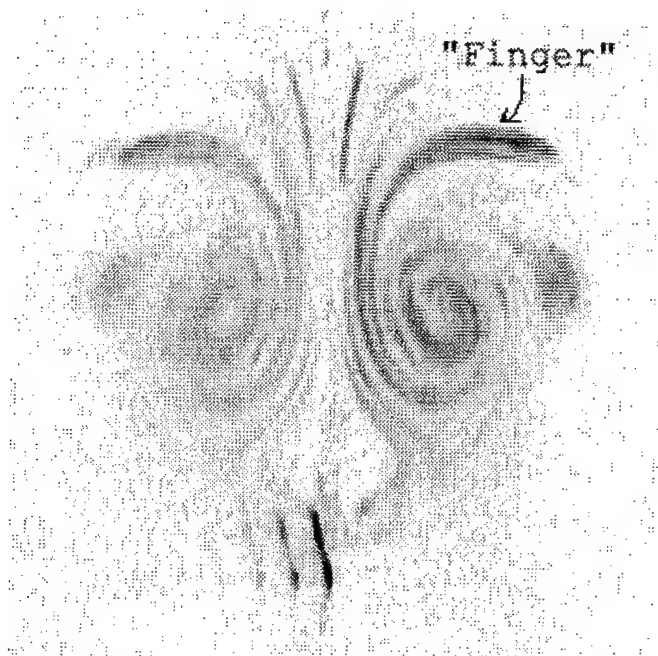
Figure 3-25: $\alpha = 30°$, x/c = 0.1, Lower Vortex

The right vortex is the actual vortex. With the delta
wing made of Plexiglas, a mirror image was created, which
is seen on the left. This vortex to the right has negative
vorticity (with clockwise rotation). An interesting note
is the "finger" that exists. This part is actually
rotating in the counter-clockwise direction, caused by a
shear layer. Shih and Ding (1996) observed similar trends.
Figures 3-26 and 3-27 give the vortex core plane view for a
30° angle of attack. Figure 3-26 has chord position 0.1c
and Figure 3-27 has chord position 0.4c. The further
downstream, the further away from the plate the vortex
filament travels.
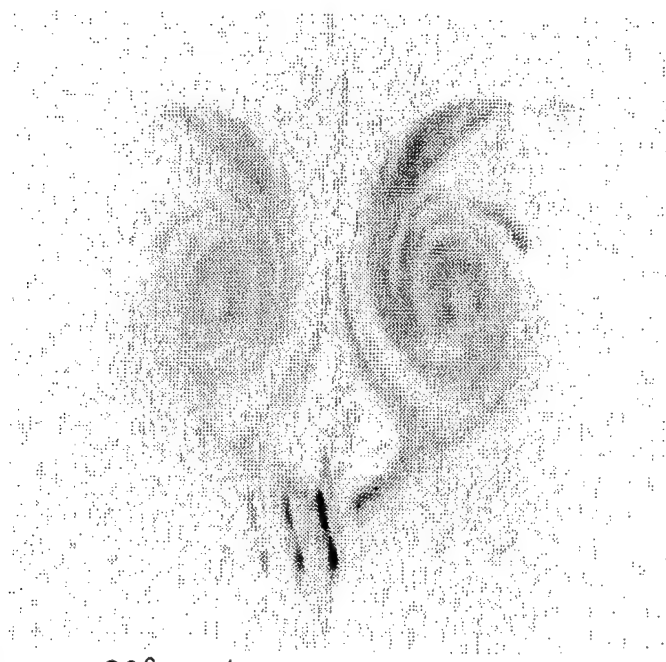
Figure 3-26: α = 30°, x/c = 0.1, Lower Vortex
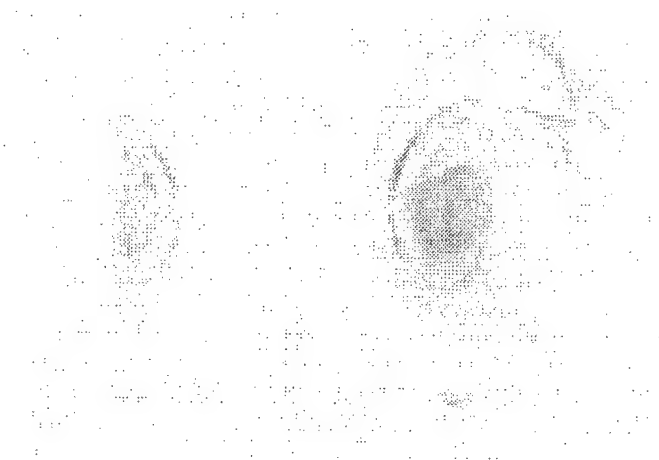
Figure 3-27: $\alpha = 30°$, $x/c = 0.4$, Lower Vortex

By measuring the distance between the two cross-view pictures and their distances away from the plate, the angle of the vortex filament off the plate was determined to be 8.2°, as shown in the following illustration.
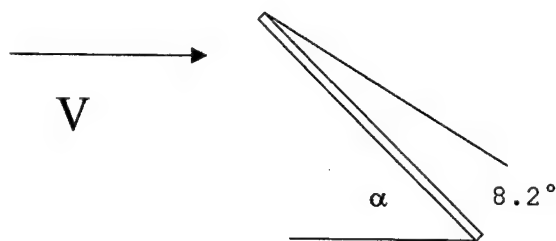
Figure 3-28: Angle of Vortex off Wing, Zero Yaw

Another important observation was the strength of the vortices when the wing is yawed. The wing was placed at 30° AOA and 30° yaw. The laser sheet was placed at 0.3c. PIV was taken on both the windward side vortex and the leeward side vortex. LIF observations showed that the

windward side vortex remained close to the plate, as it

did with zero yaw. However, the leeward side vortex was

raised even further off the plate, as shown in the

following figure.
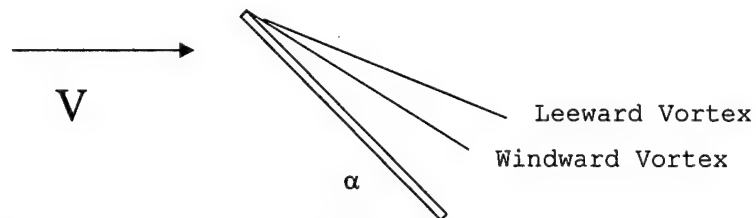
Figure 3-29: Effect of Yaw on Vortices

Because of this observation, an assumption can be made that

the windward side vortex would be stronger than the leeward

side vortex. Figures 3-30 and 3-31 show the component of

vorticity normal to the y-z plane, or ω_x, for the windward

side vortex and the leeward side vortex, respectively.
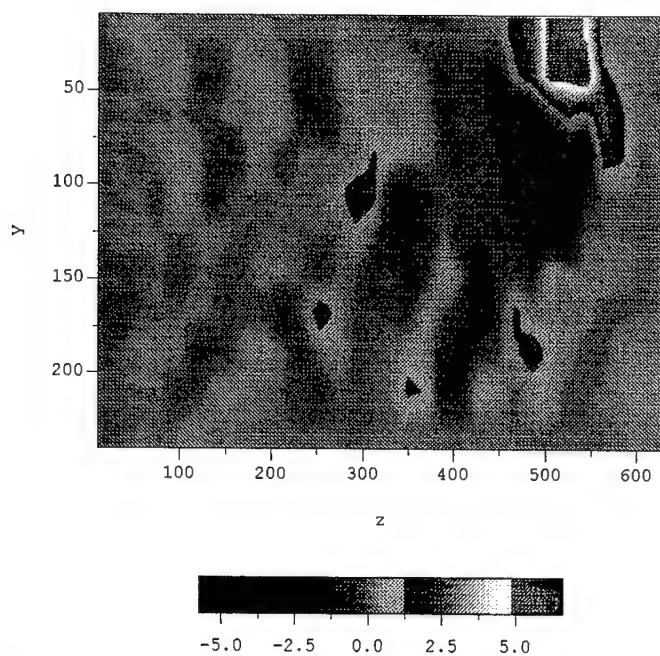
Figure 3-30: ω_x, $\alpha = 30°$, $x/c = 0.3$, Windward Side Vortex
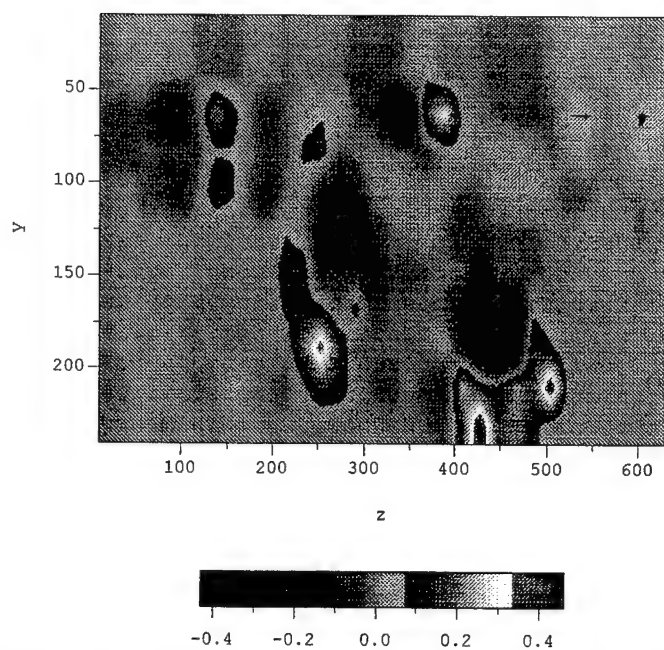
Figure 3-31: ω_x, $\alpha = 30°$, $x/c = 0.3$, Leeward Side Vortex

In figure 3-30, two strong vortices appear. The negative vortex is the vortex that is moving in the clockwise direction. This is the apex vortex. The positive vortex is moving in the counter-clockwise direction. This is a secondary vortex which is formed with the aid of a shear layer observed as the "finger" in the LIF picture of figure 3-25. A more complete discussion concerning the secondary vortices can be found in Shih and Ding (1996). The magnitude of the apex vortex is about 5.

The vortices in Figure 3-31 are harder to see. The reason for this is that it is very difficult to get rid of the noise. After collecting data, many data points can be deleted because their magnitude is beyond a certain threshold. However, this method cannot be used for all the bad data. With the help of LIF, the apex vortex was observed to be at row 75, column 250. This vortex would not appear to be the apex vortex as it is very small in diameter and in magnitude compared to the other contours in the figure. However, it is the location of the apex vortex. The magnitude of this vortex is on the order of 0.1. Even if the other vortices present in the figure are actual vortices caused by the flow, the maximum magnitude is about 0.5.

Comparing the magnitudes of the vortex strength, it is clear that the vortex on the windward side is stronger than that on the leeward side by a factor of at least 10.

For future research in studying the vortex core plane, more time-average results should be used. For the present study, computer memory and time was an issue. Time-averaging may have reduced the noise that appears in Figure 3-31. Also, similar practice with the use of the particles and the laser sheet that was considered in the core flow should be considered with the vortex core plane.

As was the problem with the core view, Spyglass Transform™ velocities may not have given accurate results with regard to the magnitude of the vortices. Recalibration is important. For the purposes of this study, general trends were observed which should aid future research.

Chapter 4: Conclusions

In this chapter, a summary of the experimental results will
be presented in addition to areas of future research.

4.1 Summary of Results

The first result was a visual observation. Two wings, with
the same leading edge but different root chords and
slightly different thicknesses, where placed at various
angles of attack to determine the location of the
breakdown. Despite the slight thickness difference, the
breakdown occurs at roughly the same distance downstream.
Therefore, it is reasonable to substitute one wing with the
other in these experiments.

With zero yaw, experimental results confirmed that
within the core of the vortex, the axial velocity speeds up
considerably until breakdown. At this point, the velocity
drops off rapidly.

By changing the yaw, results are consistent.
However, when the yaw angle is increased to a point where
the leeward side vortex leaves the plate, results are
different for the leeward side vortex. Initially, the
velocity increases rapidly, followed by a very gradual
increase in velocity. Also, a breakdown never occurs on
the leeward side after it has left the plate.

A view of the vortex core plane (the cross-view of a
vortex filament) shows that as the angle of attack
increases the strength of the vortex increases. The two
vortices, at zero yaw, have similar strengths (though
asymmetry does exist). As yaw increases, the windward side
vortex increases in strength while the leeward side vortex
decreases in strength.

4.2 Future Research

During the research for this present study, ideas were
sought as to what areas should be tested in the future.
Two ideas are a transition mount and a non-straight leading
edge.

4.2.1 Transition

Data in this study was collected as the wing was placed at a stationary angle of attack. To better analyze what happens in actual flight, the wing should operate at a pitch-up and hold condition. In addition to this study, a transition mount was created in order to change the angle of attack at a pace consistent with actual flight.

4.2.2 Non-Straight Leading Edge

All the research on vortex breakdown is based on a delta wing with straight leading edges. From flow visualization, the vortex is seen to "wrap" around the leading edge. If a non-straight leading edge is introduced, the flow will be disturbed. The question is whether it will suppress the breakdown or not. An idea for this analysis is to introduce sinusoidal shaped cuts into the leading edges.

REFERENCES

Erickson, G.E., "Vortex Flow Correlation," Technical
    Report, AFWAL-TR-80-3143, 1980.

Eroglu, A., "An Experimental Investigation of Entrainment
    and Mixing in Pulsed and Exponential Transverse Jets,"
    Ph.D. dissertation, University of Washington, 1991.

Faler, J.H. and Leibovich, S., Phys. Fluids, vol 20, pp.
    1385-1400, 1977.

Gad-el-Hak, M. and Blackwelder, R.F., "The Discrete
    Vortices from a Delta Wing," AIAA Journal, Vol. 23,
    No. 6, 1985, pp. 961-962.

Haven, B.A., "The Effect of Hole Geometry on the Near Field
    Character of Crossflow Jets," Ph.D. dissertation,
    University of Washington, 1996.

Kurosaka, M., Campbell, M. and Taya, M., "Vortex Breakdown
    Control Using Flush-Mounted Micro Adaptive Actuators,"
    Vol. I: Technical Proposal, 1998.

Lowson, M.V., Riley, A.J. and Swales, C., "Flow Structure
    over Delta Wings," AIAA Paper 95-0586, Jan. 1995.

Payne, F.M., Ng., T.T., Nelson, R.C. and Schiff, L.B.,
    "Visualization and Wake Surveys of Vortical Flow over
    a Delta Wing," AIAA Journal, Vol. 26, No. 2, 1988.

Shi, Z., Wu, J.M. and Vakili, A.D., "An Investigation of
    Leading-Edge Vortices on Delta Wings with Jet
    Blowing," AIAA Paper, Jan. 1987.

Shih, C. and Ding, Z., "Unsteady Structure of Leading-Edge
    Vortex Flow Over a Delta Wing", AIAA Paper 96-0664,
    1996

Spall, R.E., Phys. Fluids, vol. 8, pp. 1330-1332, 1996.

TSI Particle Image Velocimetry System Operation Manual,
    1995.

Yamagata, D.K., "The Influence of Anti-Kidney Pair of
    Vortices on Shaped Film Cooling Holes," Master of
    Science thesis, University of Washington, 1996.

University of Washington

Abstract

Velocity Field Over Delta Wings at High Angles of Attack

By Devin O. O'Dowd

Chairman of Supervisory Committee:
Professor Mitsuru Kurosaka
Department of Aeronautics and Astronautics

Water tunnel experiments were conducted to understand
the nature of vortex breakdown over delta wings at high
angles of attack and at various yaw angles. Two delta
wings with the same sweep angle but different chords and
slightly different thicknesses were placed inside the water
tunnel. Experiments were conducted using two techniques,
Laser Induced Fluorescence (LIF) and Particle Image
Velocimetry (PIV).

Results showed that the core flow experiences an
increase in velocity until breakdown followed by a sharp
decrease in velocity. As the angle of attack increases,
the core flow inside the vortices slows down, in general,
and the strength of the vortices increases. As yaw
increases, the windward side vortex increases in strength
and moves upstream while the leeward side vortex decreases
in strength and moves downstream. At a critical yaw angle,
the leeward side vortex leaves the plate and this vortex
neither leaves the plate, nor experiences an increase in
velocity such as the windward vortex does.

University of Washington

Abstract

Velocity Field Over Delta Wings at High Angles of Attack

By Devin O. O'Dowd

Chairman of Supervisory Committee:
Professor Mitsuru Kurosaka
Department of Aeronautics and Astronautics

Water tunnel experiments were conducted to understand the nature of vortex breakdown over delta wings at high angles of attack and at various yaw angles. Two delta wings with the same sweep angle but different chords and slightly different thicknesses were placed inside the water tunnel. Experiments were conducted using two techniques, Laser Induced Fluorescence (LIF) and Particle Image Velocimetry (PIV).

Results showed that the core flow experiences an increase in velocity until breakdown followed by a sharp decrease in velocity. As the angle of attack increases, the core flow inside the vortices slows down, in general, and the strength of the vortices increases. As yaw increases, the windward side vortex increases in strength and moves upstream while the leeward side vortex decreases in strength and moves downstream. At a critical yaw angle, the leeward side vortex leaves the plate and this vortex neither leaves the plate, nor experiences an increase in velocity such as the windward vortex does.

REFERENCES

Erickson, G.E., "Vortex Flow Correlation," Technical Report, AFWAL-TR-80-3143, 1980.

Eroglu, A., "An Experimental Investigation of Entrainment and Mixing in Pulsed and Exponential Transverse Jets," Ph.D. dissertation, University of Washington, 1991.

Faler, J.H. and Leibovich, S., Phys. Fluids, vol 20, pp. 1385-1400, 1977.

Gad-el-Hak, M. and Blackwelder, R.F., "The Discrete Vortices from a Delta Wing," AIAA Journal, Vol. 23, No. 6, 1985, pp. 961-962.

Haven, B.A., "The Effect of Hole Geometry on the Near Field Character of Crossflow Jets," Ph.D. dissertation, University of Washington, 1996.

Kurosaka, M., Campbell, M. and Taya, M., "Vortex Breakdown Control Using Flush-Mounted Micro Adaptive Actuators," Vol. I: Technical Proposal, 1998.

Lowson, M.V., Riley, A.J. and Swales, C., "Flow Structure over Delta Wings," AIAA Paper 95-0586, Jan. 1995.

Payne, F.M., Ng., T.T., Nelson, R.C. and Schiff, L.B., "Visualization and Wake Surveys of Vortical Flow over a Delta Wing," AIAA Journal, Vol. 26, No. 2, 1988.

Shi, Z., Wu, J.M. and Vakili, A.D., "An Investigation of Leading-Edge Vortices on Delta Wings with Jet Blowing," AIAA Paper, Jan. 1987.

Shih, C. and Ding, Z., "Unsteady Structure of Leading-Edge Vortex Flow Over a Delta Wing", AIAA Paper 96-0664, 1996

Spall, R.E., Phys. Fluids, vol. 8, pp. 1330-1332, 1996.

TSI Particle Image Velocimetry System Operation Manual, 1995.

Yamagata, D.K., "The Influence of Anti-Kidney Pair of Vortices on Shaped Film Cooling Holes," Master of Science thesis, University of Washington, 1996.

REFERENCES

Erickson, G.E., "Vortex Flow Correlation," Technical
    Report, AFWAL-TR-80-3143, 1980.

Eroglu, A., "An Experimental Investigation of Entrainment
    and Mixing in Pulsed and Exponential Transverse Jets,"
    Ph.D. dissertation, University of Washington, 1991.

Faler, J.H. and Leibovich, S., Phys. Fluids, vol 20, pp.
    1385-1400, 1977.

Gad-el-Hak, M. and Blackwelder, R.F., "The Discrete
    Vortices from a Delta Wing," AIAA Journal, Vol. 23,
    No. 6, 1985, pp. 961-962.

Haven, B.A., "The Effect of Hole Geometry on the Near Field
    Character of Crossflow Jets," Ph.D. dissertation,
    University of Washington, 1996.

Kurosaka, M., Campbell, M. and Taya, M., "Vortex Breakdown
    Control Using Flush-Mounted Micro Adaptive Actuators,"
    Vol. I: Technical Proposal, 1998.

Lowson, M.V., Riley, A.J. and Swales, C., "Flow Structure
    over Delta Wings," AIAA Paper 95-0586, Jan. 1995.

Payne, F.M., Ng., T.T., Nelson, R.C. and Schiff, L.B.,
    "Visualization and Wake Surveys of Vortical Flow over
    a Delta Wing," AIAA Journal, Vol. 26, No. 2, 1988.

Shi, Z., Wu, J.M. and Vakili, A.D., "An Investigation of
    Leading-Edge Vortices on Delta Wings with Jet
    Blowing," AIAA Paper, Jan. 1987.

Shih, C. and Ding, Z., "Unsteady Structure of Leading-Edge
    Vortex Flow Over a Delta Wing", AIAA Paper 96-0664,
    1996

Spall, R.E., Phys. Fluids, vol. 8, pp. 1330-1332, 1996.

TSI Particle Image Velocimetry System Operation Manual,
    1995.

Yamagata, D.K., "The Influence of Anti-Kidney Pair of
    Vortices on Shaped Film Cooling Holes," Master of
    Science thesis, University of Washington, 1996.